CONCRETE FILLED FRP TUBE COLUMNS LONGITUDINALLY REINFORCED WITH FRP AND STEEL BARS

Abdeldaim Ahmed, Asmaa[1], and Masmoudi, Radhouane [2]*
[1&2] Department of Civil Engineering, University of Sherbrooke, Qc, Canada
* Corresponding author (Radhouane.Masmoudi@USherbrooke.ca)

Keywords*: FRP; Concrete-filled tube; Columns*

ABSTRACT

Infrastructure safety, durability, and serviceability have been significantly enhanced as a result of improved construction materials over the past two decades. Concrete-filled fibre-reinforced polymer (FRP) tubes (CFFTs) system is one of the most promising technique to protect the reinforced concrete structures from aggressive environmental conditions. Most of the experimental investigations performed on CFFT columns have focused on short, unreinforced, small-scale concrete cylinders, tested under monotonic axial loading. In contrast, only few studies have so far investigated the effects of the internal longitudinal reinforcement type (steel or FRP bars) on the behavior of CFFT long columns. This paper presents preliminary test results of an experimental study on the behaviour of concrete-filled FRP tube (CFFT) columns internally reinforced with steel and FRP bars. Six reinforced concrete (RC) and CFFT columns were constructed and tested until failure. The test parameters were: (1) internal reinforcement type (steel, glass FRP (GFRP), and amount, and (2) GFRP tube thicknesses. All columns had 1900-mm in height and 213-mm in diameter. Examination of the test results has led to a number of significant conclusions in regards to the trend and ultimate condition of the axial stress-strain behaviour and mode of failure of tested CFFT columns. These results are presented, and a discussion is provided on the influence of the main test parameters in the observed behaviours.

1 INTRODUCTION

An important application of fibre-reinforced polymer (FRP) composites is as a confining material for concrete, both in the seismic retrofit of existing reinforced concrete (RC) columns and in the construction of concrete-filled FRP tubes (CFFTs) as earthquake-resistant columns in new construction. The FRP tube acts as a stay-in-place structural formwork, a noncorrosive reinforcement for the concrete for flexure and shear using the multidirectional fiber orientation, provides confinement to the concrete in compression, and the contained concrete is protected from intrusion of moisture with corrosive agents that could otherwise deteriorate the concrete core [2].

To date, most of the experimental investigations performed on FRP confined concrete columns have focused on short, unreinforced, small-scale concrete cylinders, tested under concentric and monotonic axial loading [7, 3, 5, 11, 15]. In contrast, only few studies have so far investigated the effects of the slenderness ratio and internal longitudinal reinforcement type (steel or FRP bars) on the behavior of FRP confined concrete long columns [7, 8, 4, 6, 17]. Mirmiran et al [7] carried out a comprehensive parametric study on the buckling of over 11 500 CFFT columns. They found that instability of CFFT columns might occur at a lower slenderness ratio than that of ordinary RC columns

(without FRP tubes); however, the ultimate capacity of the former might be higher than that of the latter. This attributed to the bilinear stress-strain behavior of the CFFT columns in which the buckling mode of failure initiated at the plastic branch of the curve, which was characterized by a lower Young's modulus. They also recommended that the current slenderness limit of 22 for steel-reinforced concrete columns bent in single curvature be reduced to 11 for CFFT columns. Masmoudi and Mohamed [6] conducted an experimental investigation on the axial behavior of CFFT columns internally reinforced with steel or carbon FRP (CFRP) bars with different slenderness ratios ranging from 4 to 20. The test results showed that the CFFT columns reinforced with CFRP bars behaved similar to that of CFFT columns reinforced with steel bars. The axial capacity of steel or CFRP-reinforced CFFT decreased as the slenderness ratios increased. This can draw the conclusion that the increase of the slenderness ratio of CFFT columns reinforced internally with steel or CFRP bars might be a critical factor that controls the mode of failure and might prevent such columns from attaining their ultimate load capacity.

To the knowledge of the candidate, no investigations have addressed the behavior of FRP-reinforced CFFT columns under axial cyclic compression loading. To address such knowledge gaps and properly understanding the general behavior of FRP-reinforced CFFT columns under axial cyclic loading more experimental studies are needed. This paper presents the test results of an experimental study aimed at investigating the behavior of CFFT columns reinforced with longitudinal steel or FRP bars tested under axial cyclic compression loading. A total of six RC and CFFT columns were constructed and tested until failure. All columns had 1900-mm in height and 213-mm in diameter. The effect of internal reinforcement type and amount, and GFRP tube thicknesses were addressed.

2 EXPERIMENTAL WORK

2.1 Materials

Four materials were used in fabricating the test specimens. These materials are concrete, FRP tubes, steel reinforcing (bars and stirrups), and FRP bars. The following sections provide a description of the different experimental tests conducted to evaluate the mechanical properties of the different materials used herein.

2.1.1 Concrete

All columns were constructed using a ready-mixed normal strength concrete (NSC) with an entrained-air ratio of 5% to 8%. The actual concrete compressive strength was determined from testing six concrete cylinders (150 × 300 mm) on the same day of testing the columns. **Error! Reference source not found.** shows typical axial stress-strain curves for the concrete cylinders. The average concrete compressive strength and tensile strength were 41.5 MPa and 4.2 MPa, respectively.

2.1.2 Steel and FRP bars

Two different steel bars were used to reinforce the control and CFFT specimens. Wire mild steel bars 3.4 mm in-diameter were served as transverse spiral reinforcement for the control specimens. Deformed steel bars M15 (16 mm in diameter; 200 mm2 in cross-sectional area); were used as a longitudinal reinforcement for test specimens. The mechanical properties of the steel bars obtained from standard tests that were carried out according to ASTM [1], on five specimens for each type of the steel bars. The mechanical properties of the steel bars are presented in Table 1. Two types of sand-coated FRP bars manufactured by a Canadian company [12] were used as longitudinal reinforcement for the tested columns. Sand-coated surface was made to improve the bond between the bars and surrounding concrete. The two types of FRP bars were made from continuous glass fibres with a fibre content of 73% and impregnated in a vinyl ester resin through the pultrusion process. GFRP bars No. 3 and No. 5 (9.5 mm and 15.9

mm in-diameter; 71 mm2 and 199 mm2 in cross-sectional area, respectively) were used. Table 1 shows the mechanical properties of the FRP bars as provided by the manufacture. Figure 2 shows the different bars used in this investigation.

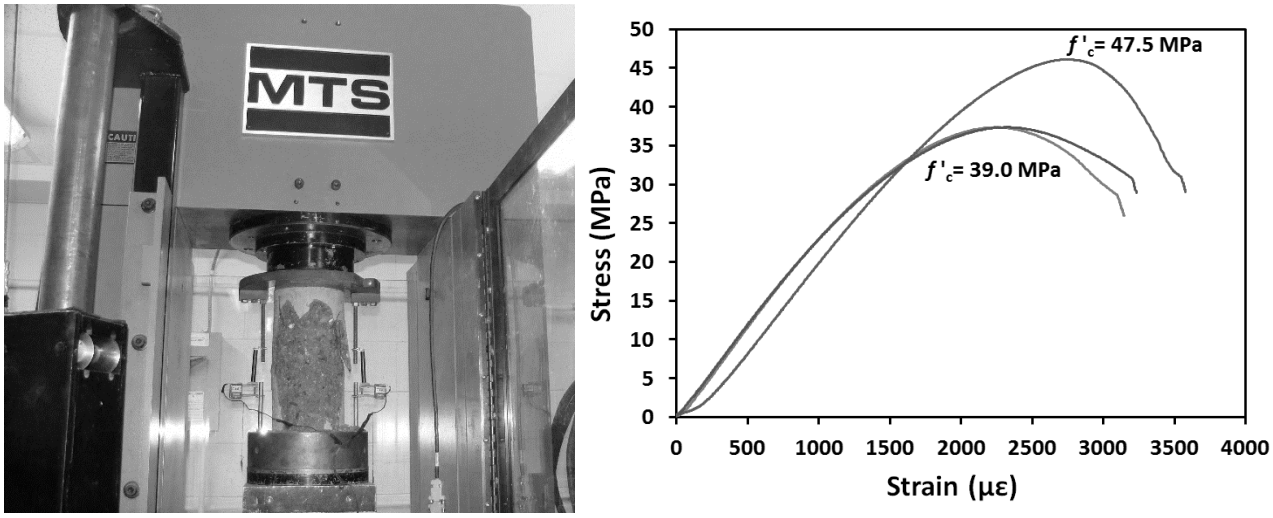

Figure 1. Typical axial stress-strain relationships for concrete cylinders

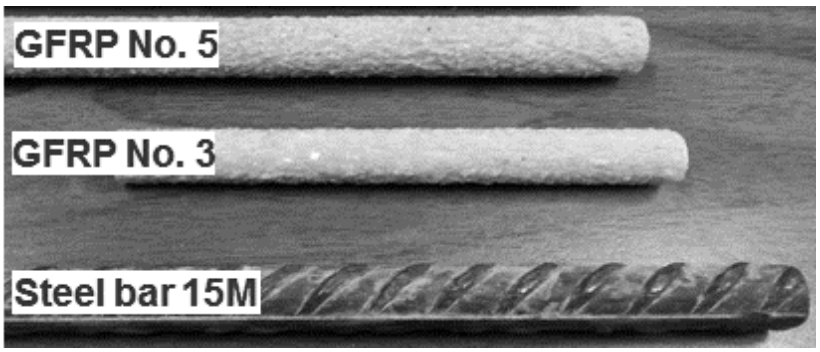

Figure 2. Different steel and FRP bars used in this study

Reinforcement type	Nominal diameter (mm)	Nominal area (mm²)	Tensile modulus of elasticity (GPa)	Yield strength (MPa)	Ultimate strength (MPa)	Ultimate strain (%)
GFRP	9.5	71	45.4	-	856	1.89
	15.9	199	48.2	-	751	1.60
Wire (mild steel)	3.4	9	200	675	850	0.30*
15M (deformed)	16	200	200	419	686	0.21*

* Yield strain

Table 1. Tensile properties of the GFRP, and steel bars

2.1.3 FRP tubes

Two types of GFRP tubes were used as structural stay in-place formwork for the tested specimens herein. The GFRP tubes were fabricated using filament-winding technique; E-glass fiber and Epoxy resin were used for manufacturing these tubes. The two types of GFRP tubes (types A&B) were used with different thicknesses and having the same internal diameters 213 mm. The thickness of tube (A) equals 2.90 mm, while for tube B equals 6.40 mm. Different fibre angles with respect to the longitudinal axis of the tubes were used (±60°, ±65°, ±45°, and 90°). The fibre orientations of the tubes were mainly in the hoop direction, and no fibres in the longitudinal direction. The glass fibre volume fraction as provided by the manufacture was 68% ± 3%. Figure 3 shows the specimens of FRP tubes for the split-disk test and coupon tensile test. Typical test samples of the coupon tests and split-disk test in the hoop direction for GFRP tubes are shown in Figures 4 and 5, respectively. Table 2 shows the dimensions and mechanical properties of FRP tubes.

Tube type	D (mm)	t_{frp} (mm)	No. of layers	Stacking sequence	f_{FRPU} (MPa)	ε_{FRPU} (%)	E_{FRPU} (MPa)	f_X (MPa)	ε_X (%)	E_X (MPa)
A	213	2.90	6	[60 º, 90 º, 60 º]	548	1.70	32260	55.2	0.62	8865
B	213	6.40	12	[±60 º, 90 º, ±60 º, 90 º]	510	1.69	30200	59.2	0.75	7897

D and t_{frp} are the internal diameter and thickness of the FRP tubes, respectively. f_{FRPU}, ε_{FRPU}, and E_{FRPU} are, respectively, the ultimate strength, ultimate tensile strain, and Young's modulus in the hoop direction; while f_X, ε_X, and E_x are the ultimate strength, ultimate tensile strain, and Young's modulus in the axial direction, respectively.

Table 2. Dimension and mechanical properties of FRP tubes

2.2 Instrumentation and testing procedures

Several strain gauges were mounted on the internal reinforcement bars prior the concrete casting and on concrete or GFRP tube surfaces before testing. Eight strain gauges were located at the column mid-height in both axial and lateral directions to measure the axial and lateral strains, respectively. Two strain gauges were bonded on two longitudinal bars at 180º degree apart at the mid-height of the column. Figure 6 (a) shows the strain gauges instrumentation GFRP tube surface. Two displacement transducers (DTs) were used to measure the axial deformation of the column over the full height as shown in Figure 6 (a). Additionally, two in-plane linear variable displacement transducers (LVDTs) were located at the mid-height to record the lateral displacements of each column. All columns were capped with a thin layer of the high strength sulphur to ensure uniform load distribution during testing. Before testing, both ends of the columns were further confined with bolted steel collars made from 10 mm thick steel plates in order to prevent premature failure at their ends. The specimens were loaded under axial compression loading using a 6000-kN capacity-testing machine. Loading and unloading in compression tests were achieved with load control at a rate approximately equal to 2.3 kN/s. During the test, load, axial and lateral displacements, and strain gauges were recorded automatically using a data acquisition system connected to the computer. Figure 6 (b) shows the test specimen inside the testing machine.

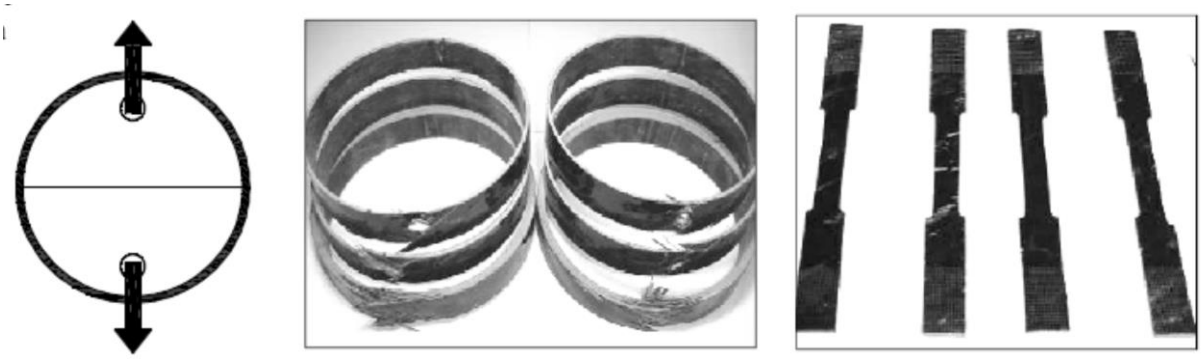

Figure 3. Specimens of FRP tubes for the split-disk test and coupon tensile test [6]

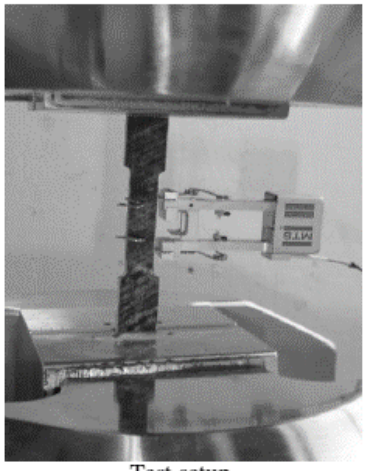

Test setup

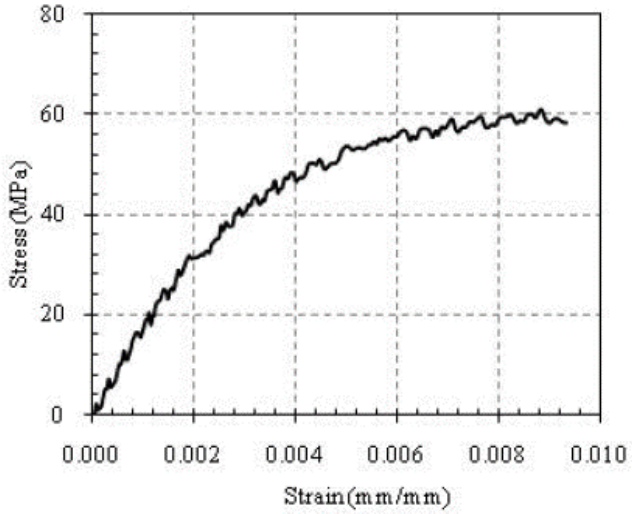

Figure 4. Test setup and load-strain curve for the FRP tubes for coupon tensile test [6

Test Setup

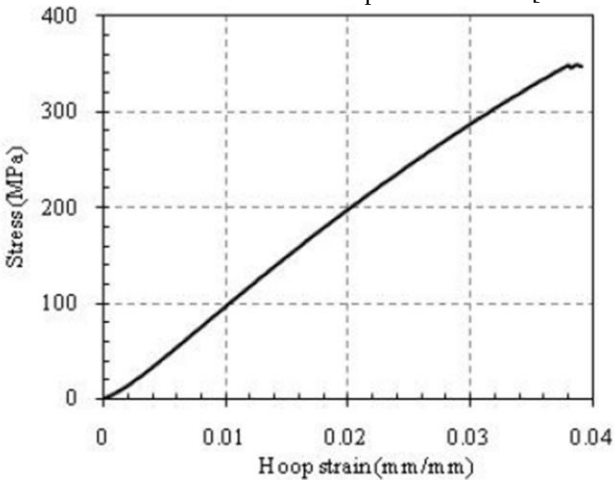

Figure 5. Test setup and stress-hoop strain behaviour of the FRP tubes for split-disk test [6]

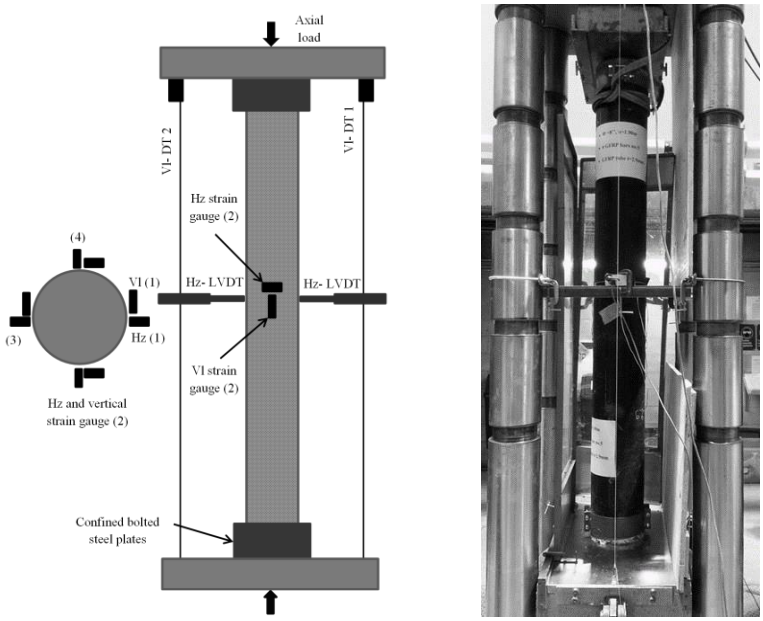

(a) (b)

Figure 6. Instrumentations and Test setup: (a) schematic of the test setup and placing of specimen instrumentations; (b) test specimen inside the testing machine

2.3 Test specimens

A total of six RC and CFFT circular columns were fabricated and tested under concentric axial cyclic compression loading. Two RC control columns and four CFFT columns were internally reinforced with steel, or Glass FRP (FRP). The test parameters were: (i) GFRP tubes thicknesses (2.9 and 6.4 mm); and (ii) internal reinforcement type (steel; and GFRP) and amount. All columns had the same height (h=1900 mm) to diameter (D=213 mm) ratio of 9.0. The control RC columns were reinforced longitudinally with reinforcement ratio (ρ_L) equal to (3.4%), one specimen reinforced with steel bars and the other specimen reinforced with GFRP bars. Steel spiral stirrups (pitch = 50.6 mm) were used as transverse reinforcement and designed to have approximately similar hoop stiffness as the GFRP tube (Type A). The CFFT columns were laterally confined with GFRP tubes (Type A or B). One specimen was internally reinforced with deformed steel bars (6 M15; ρ_L = 3.4%) and laterally confined with tube type (A). Three specimens were reinforced with 6 GFRP bars No. 3 or No. 5 (ρ_L = 1.2 and 3.4%, respectively) and laterally confined with tubes type (A and B). The test specimens were labeled as follows: the first letter S, A, or B is defining "the type of lateral reinforcement: steel spiral stirrups, GFRP tube type (A), or tube type (B)" then followed by a letter S, or G indicating "the longitudinal reinforcement type: steel, or GFRP bars", respectively. The number between brackets indicates "the longitudinal reinforcement ratio". The final letter (C) refers to unloading/reloading cyclic loading. Table 4 shows the test specimens' details.

3 TEST RESULT

3.1 Axial and Lateral Stress-Strain Responses

As shown in Figure 7 the stress-strain responses of the GFRP-reinforced control columns behaved similar to that of the steel-reinforced control column up to their peak load. However, the peak axial stress for steel-reinforced column was slightly higher than that of their counterpart reinforced with GFRP bars by 11% (on average). The axial stress-

strain curves for GFRP and steel reinforced CFFT columns showed similar shapes of the hysteresis loops for the unloading/reloading paths. However, the steel-reinforced CFFT column hysteresis loop starts to open after the yielding of steel bars. The unloading paths for the CFFT columns reinforced with steel or FRP bars exhibited non-linear behavior. The degree of the non-linearity increases as the unloading axial strain increases. The reloading paths can be resembled as straight lines. The envelop curves of the reinforced CFFT- columns, representing the upper boundary of the axial cyclic stress-strain responses, showed bilinear responses with a transition zone in the vicinity of the unconfined concrete (fc') followed by nearly stabilization of the load carrying capacity as shown in specimens B-$G_{(3.4)}$-C and B-$G_{(1.2)}$-C). The initial slope was almost identical for all the specimens while the second slope is highly governed by GFRP tubes stiffness rather than the internal reinforcement type and amount, particularly in thicker tube thickness.

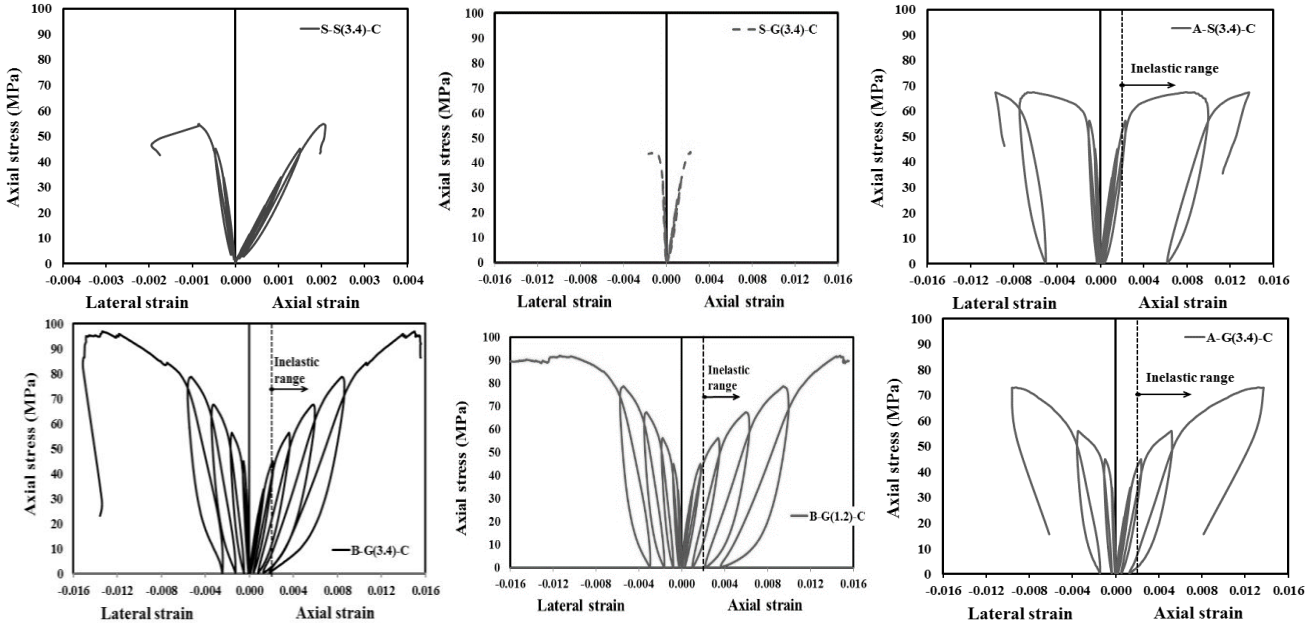

Figure 7. Axial and lateral stress-strain curves of the tested specimens

3.2 State of Stress in the Fiber Reinforced Polymer Tube

Typical distributions of axial and lateral strains at various loads of selected reinforced CFFT columns over the perimeter of the GFRP tube at the column mid-height are presented in Figure 8. As shown in this figure, the uniform distribution of the lateral strains in the FRP tubes near loading level of 2000 kN indicates efficient confinement of the tubes. As a result of the instability failure of the reinforced CFFT columns due to buckling produced highly variable lateral confinement and induced significant bending in the column before failure. The maximum, minimum, and average lateral strains in the hoop direction (εh,max, min, aver.) of the FRP tube at the ultimate load are reported in Table 4.

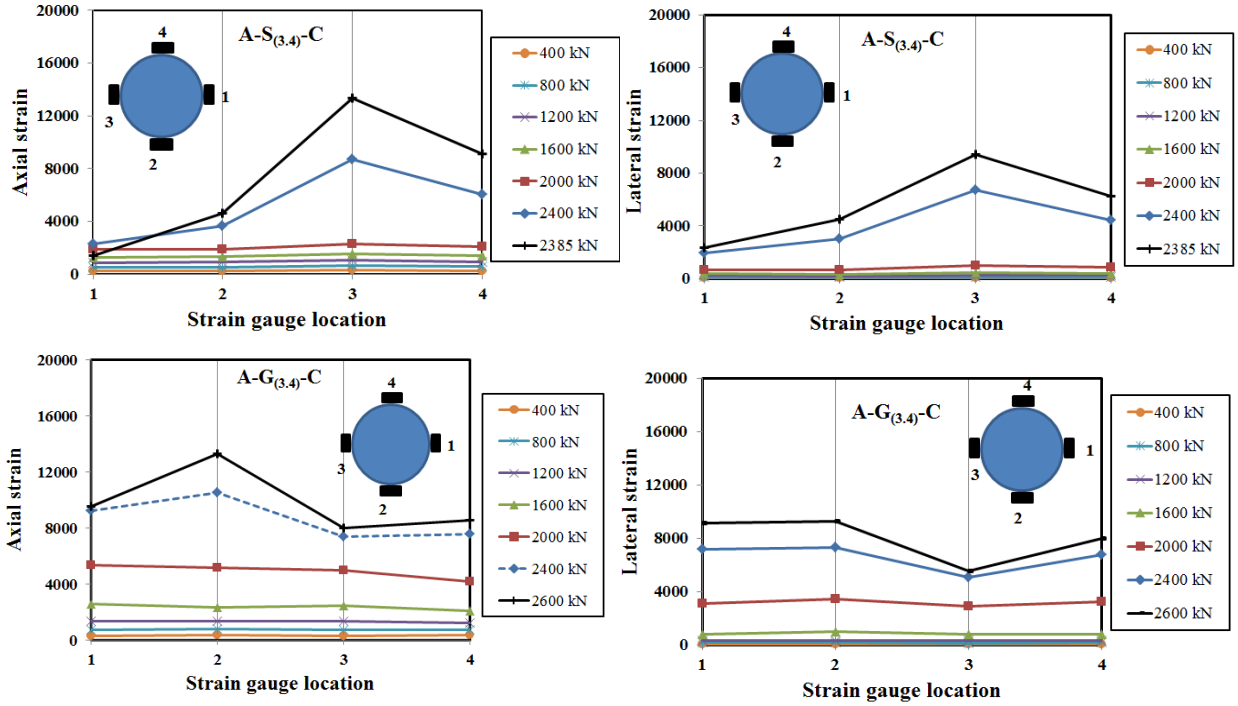

Figure 8. Strain distribution versus different strain gauges locations surrounding the column perimeter at the mid-height for specimen A-S(3.4)-C and A-G(3.4)-C

ID	Lateral reinforcement type	Longitudinal bars		P u (kN)	f'_{cc} (MPa)	f'_{cc}/f'_{c}	εcc (με)	$\varepsilon_{cc}/\varepsilon_{o}$	εh, min. (με)	εh, aver. (με)	εh, max. (με)
		Type	Area								
S-S(3.4)-C	ϕ3.4@50.6	Steel	6 M 15	1948	54.60	1.23	-2510	1.04	377	599	836
S-G(3.4)-C	ϕ3.4@50.6	GFRP	6 No. 5	1575	47.20	1.08	-2711	1.12	653	935	1144
A-S(3.4)-C	A	Steel	6 M 15	2402	67.38	1.53	-13749	3.83	2442	4697	9707
A-G(3.4)-C	A	GFRP	6 No. 5	2603	73.06	1.66	-13718	4.63	5172	8087	9610
B-G(3.4)-C	B	GFRP	6 No. 5	3455	96.97	2.20	-15578	5.49	4435	9745	15135
B-G(1.2)-C	B	GFRP	6 No. 3	3272	91.82	2.08	-15563	5.96	11456	13787	16113

Table 4. Specimen's details and test results

3.3 Axial load carrying capacity

The strength and strain enhancement ratios of the CFFT columns (A-$S_{(3.4)}$-C and A-$G_{(3.4)}$-C) were increased ranging from 1.3 to 1.5 and 3.7 to 4.4 times compared to their counterpart control specimens (S-$S_{(3.4)}$-C and S-$G_{(3.4)}$-C), respectively as indicates in Table 4. Providing the FRP tube as in tube A enhanced the strength and strain capacity by 52% and 470%, respectively, in comparison with their control specimens which were reinforced with steel spiral stirrups and designed to have similar lateral stiffness as in Tube A. This can be attributed to the continuity of the FRP tubes rather than the discontinuity of the steel stirrups, which reflects the superior confining behavior of the FRP tubes over the steel stirrups to increase not only the strength but also the ductility of the CFFT columns [8]. Increasing the

GFRP tube thickness from 2.9 to 6.4 mm enhanced both the strength and strain ratios by 25% and 12%, respectively. This can be attributed to the enhancement of lateral confinement, as a result of increasing the stiffness of the tube.

3.4 Failure mode

The GFRP tube provided significant confinement attributing to shift the failure mode from axially dominated material failure to instability failure for the CFFT columns. The instability was evident in a significant single curvature mode shape of the bent column. Despite, the specimens experienced much lateral deflections beyond the ultimate load, the deflected columns were still stable and carried more axial load. Loading the specimens continued until localized failure occurred near the mid height of the column. Finally, GFRP tube rupture, concrete crushing, and local buckling of steel bars or crushing of the FRP bars in the compression side of the CFFT columns were observed. This observation is in agreement with the previous research works conducted on slender FRP-confined columns [8, 4]. On the other hand, the control columns showed substantially different failure mode compared to that occurred for the CFFT columns. For both control columns reinforced with steel or GFRP bars showed similar responses. The failure was typically initiated with vertical cracks started to appear at approximately 85% of their peak loads and followed by concrete dilation and lateral deformation of transverse and longitudinal reinforcement leading to concrete cover spalling. Thereafter, the concrete core crushed and spiral stirrups fractured after buckling of the longitudinal bars. Moreover, inclined diagonal shear surface was observed leading to a separation of the concrete core into two column parts causing a sudden drop after reaching the peak load. **Error! Reference source not found.** shows Overall failure modes of tested specimens. Table 4 summarizes the test results for all specimens.

Figure 9. Overall failure modes of tested specimens

4 CONCLUSIONS

Based on the experimental test results and discussions, the following conclusions can be drawn:

1. Increasing the thickness of the GFRP tubes significantly increased the ultimate axial and strain capacities of the CFFT reinforced tested columns.
2. The CFFT columns reinforced with GFRP bars exhibited similar responses compared to their counterparts reinforced with steel bars at the same longitudinal reinforcement amount. No significant difference was observed in terms of ultimate axial strength and strain capacities.
3. Using FRP bars instead of conventional steel bars in the CFFT columns can provide a step forward to develop a totally corrosion-free new structural system.

5 REFERENCES

[1] ASTM A615/A615M-09, ASTM 2009. Standard specification for deformed and plain carbon steel bars for concrete reinforcement, West Conshohocken, Pa.

[2] American Concrete Institute (ACI), (2008), "Guide for the design and construction of externally bonded FRP systems for strengthening concrete structures." ACI 440.2R-08, Farmington Hills, Mich.

[3] Fam, A., Greene, R. and Rizkalla, S. 2003. Field Applications of Concrete-Filled FRP Tubes for Marine Piles. ACI Special Publication, (Field Application of FRP Reinforcement: Case Studies) SP(215)9:161-180.

[4] Fitzwilliam, J and Bisby, L. 2010. Slenderness Effects on Circular CFRP Confined Reinforced Concrete Columns. Journal of Composites for Construction, 14(3): 280-288.

[5] Lam, L., and Teng, J. G. 2009. Stress-strain model for FRP-confined concrete under cyclic axial compression. Eng. Struct., 31(2):308–321.

[6] Masmoudi, R. and Mohamed, H. 2011. Axial behavior of slender-concrete-filled FRP tube columns reinforced with steel and carbon FRP bars. 10th International Symposium on Fiber-Reinforced Polymer Reinforcement for Concrete Structures, Tampa, Florida, April 2011, ACI-SP-275.

[7] Mirmiran, A.; Shahawy, M.; and Beitleman, T. 2001. Slenderness Limit for Hybrid FRP Concrete Columns. Journal of Composites for Construction, ASCE, 5(1): 26-34.

[8] Mohamed, H., Abdel Baky, H. and Masmoudi, R., 2010, "Nonlinear stability analysis of CFFT columns: Experimental and Theoretical Investigations", ACI Structural Journal, V. 107, No. 6, pp. 699-708.

[9] Mohamed, H.; Afifi, M.; and Benmokrane, B. 2014. Performance Evaluation of Concrete Columns Reinforced Longitudinally with FRP Bars and Confined with FRP Hoops and Spirals under Axial Load. the Journal of Bridge Engineering, © ASCE, ISSN /04014020(12) :1084-0702.

[10] Ozbakkaloglu, T., and Akin, E. 2012. Behavior of FRP-confined normal- and high-strength concrete under cyclic axial compression. J. Compos. Constr, 2012(16):451-463.

[11] Ozbakkaloglu, T, Lim, J, Vincent, T. 2013. FRP-confined concrete in circular sections: Review and assessment of stress–strain models. Engineering Structures 49:1068–1088.

[12] Pultrall, Inc. 2007. V-ROD Composite Reinforcing Rods Technical Data Sheet. Thetford Mines, Canada, www.pultrall.com.

[13] Shao, Y., Zhu, Z., and Mirmiran, A. 2006. Cyclic modeling of FRP confined concrete with improved ductility. Cem. Concr. Compos., 28(10): 959–968.

[14] Theodoros R. 2001. Experimental investigation of concrete cylinders confined by carbon FRP sheets, under monotonic and cyclic axial compression load. Research Report. Publication 01: 2. Division of Building Technology, Chalmers University of Technology.

[15] Vincent, T. and Ozbakkaloglu T. 2014. Influence of Slenderness on Stress-Strain Behavior of Concrete-Filled FRP Tubes: Experimental Study. Journal of Composites for Construction, © ASCE, ISSN 1090-0268/04014029(13).

[16] Wang, Z; Wang, D.; Smith, S., Lu, D., 2012. CFRP-Confined Square RC Columns. II: Experimental Investigation. the Journal of Composites for Construction, 16(2). ©ASCE, ISSN 1090-0268/2012/2- 150–160.

[17] Yuan, W., and Mirmiran, A., 2001. Buckling Analysis of Concrete- Filled FRP Tubes. International Journal of Structural Stability and Dynamics, 1(3):367-383.